Steering protein and lipid digestibility by oleogelation with protein aerogels

ARTICLE

Steering protein and lipid digestibility by oleogelation with protein aerogels

Received 00th January 20xx,
Accepted 00th January 20xx

DOI: 10.1039/x0xx00000x

Stella Plazzotta[a], Marilisa Alongi[a], Lorenzo De Berardinis[a], Sofia Melchior[a], Sonia Calligaris[a*] and Lara Manzocco[a]

The aim of the present work was to assess the effect of an innovative oleogelation strategy, the aerogel-template approach, on lipid and protein digestibility. Whey protein isolate (WP) was converted into aerogel particles *via* supercritical-CO_2-drying. Oleogels were then prepared by absorption of sunflower (SO) or flaxseed (FLX) oil (80% w/w) into the aerogel particle template and subjected to *in vitro* digestion. The lipolysis degree of SO (75%) and FLX (50%) oil in oleogels resulted higher than that of the unstructured SO (65%) and FLX (24%) oils. This behaviour was attributed to the peculiar de-structuring behaviour of WP aerogel-templated oleogels upon digestion. Confocal micrographs actually demonstrated that the original oleogel structure was lost at gastric level with release of oil droplets stabilised by the undigested WP aerogel. As a result, the oil contained in the oleogel was delivered in the small intestine in the form of dispersed droplets, smaller than those observed for the unstructured oils, thus offering a larger surface for intestinal lipolysis. This was also confirmed by dynamic light scattering, showing a shift towards smaller size in digestive micelle distribution of oleogels at the end of the intestinal phase. The higher gastric resistance of WP aerogels (protein digestibility < 50%) was confirmed by Sodium Dodecyl Sulphate PolyAcrylamide Gel Electrophoresis (SDS-PAGE) and bicinchoninic acid (BCA) assay. Oleogelation through the WP aerogel-template approach could be thus regarded as a strategy to steer lipid digestibility while also modulating the release of bioaccessible peptides.

1 Introduction

The growing incidence of diet-related diseases has fostered the research of strategies to increase the health profile of foods. One of the most timely strategy in the development of healthier food is the design of food architectures steering the de-structuring behaviour of the matrix during digestion, and thus the release and absorption of nutrients.

Among innovative food structures, aerogels are a special type of food-grade nanostructured material, characterised by high porosity, extremely low density, and huge internal surface [1]. These features make aerogels perfect candidates for the engineering of ingredients able to load high amounts of gaseous or liquid molecules. In particular, liquid edible oils can be loaded into protein aerogels in amounts ranging from 0.2 to 5.6 g oil/g aerogel, depending on the loading procedure [2,3].

Protein aerogel production requires the initial heat-induced gelation of the protein aqueous solution, which causes protein unfolding and subsequent aggregation, due to the exposure of sulfhydryl and hydrophobic groups. In the following preparation step, water in the hydrogel is substituted with ethanol, which is then removed from the polymeric network by a continuous flow of CO_2 in the supercritical state, leading to a porous template [3].

[a] *Department of Agricultural, Food, Environmental and Animal Sciences, University of Udine, Udine, Italy*
**Corresponding author: sonia.calligaris@uniud.it*

Oil absorption into whey protein (WP) aerogel particles by simple mixing seems particularly promising for food applications. In our previous work, this easy loading procedure was used to produce oleogels, *i.e.*, gels entrapping large amounts of liquid oil [4,5]. The obtained oleogels contained 80% oil and had a peculiar plastic structure, similar to that of traditional hard fats, thus showing high potentialities as innovative ingredients for the production of low-saturated fat foods. This peculiar plastic behaviour was attributed to the ability of WP aerogel particles to entrap the oil through different mechanisms: the oil was not only absorbed into the pores driven by capillary forces, but also immobilized in the spaces among the particles, leading to a deformable network based on weak hydrophilic interactions [4].

Recent findings have demonstrated that oleogelation can be exploited to steer lipid digestibility [6–10]. The latter mainly occurs at the intestinal level, where the lipids are emulsified by the action of bile salts, thus facilitating the hydrolytic activity of lipases. The released free fatty acids are then included in mixed micelles and subsequently absorbed by the duodenal enterocytes [11]. When oleogels were obtained by oil structuring with lipid-soluble gelators (e.g., waxes, monoglycerides, phytosterols, ethylcellulose) a decrease of lipid digestibility was observed as compared to unstructured oil [6–10]. Lipolysis reduction was attributed to the ability of the gelator network to hinder the activity of lipolytic enzymes. Lipolysis resulted

dependent on the oleogel structure, with lipolysis extent decreasing with increasing oleogel structuration [10].

By contrast, no indication is currently reported in the literature about lipolysis of oleogels obtained *via* the protein aerogel-template approach. Supporting information can be however retrieved from literature relevant to the study of lipolysis in complex protein matrices containing oil. In this regard, opposite effects have been reported depending on the matrix structure and protein physical state. In oil-in-water emulsions stabilized by WPs, an increase in lipolysis kinetics and ratio was observed as compared to non-emulsified oil, thanks to the formation of small droplets offering a larger interfacial area available for lipase adsorption [12–14]. However, when the WPs in the emulsion continuous phase were gelled, a significant lipolysis reduction was observed, due to the ability of the protein network to reach the intestinal environment being only partially digested, thus sterically hindering lipase action [12]. Similarly, aerogelation resulted in the increase of WP gastric resistance, which has been exploited in the engineering of aerogel-based delivery systems, able to protect the loaded compounds through the harsh gastric environment [2]. Such aerogel resistance was attributed to the modifications suffered by the proteins during the different steps of the aerogel preparation, leading to a complex protein network, which hinders the action of gastric pepsin [2].

This study aims at assessing the effect of the complex structure of oleogels obtained through the aerogel template approach on the digestibility of the loaded lipids and of the aerogel proteins. To this purpose, the gastrointestinal digestion of oleogels obtained by absorption of edible oils into WP aerogel particles was simulated through an *in vitro* protocol and compared to that of the unstructured oils by determining the free fatty acid release. Sunflower (SO) and flaxseed (FLX) oils were used as loading target oils, the former being widely used in the food sector and the latter having an interesting fatty acid profile, rich in ω-3 [15]. The hydrolysis of the protein aerogel template was also assessed to have an insight into the effect of aerogelation on protein digestibility**.**

2 Material and Methods

2.1 Materials

Whey protein isolate (WP, 94.7% protein content; 74.6% β-lactoglobulin, 23.8% α-lactalbumin, 1.6% bovine serum albumin) was purchased from Davisco Food International Inc. (Le Sueur, MN, USA). Flaxseed (FLX) and sunflower (SO) oil were purchased in a local market. CO_2 (purity 99.995%,) was purchased from Sapio (Monza, Italy). P_2O_5 was purchased from Chem-Lab NV (Zedelgem, Belgium). Agar technical (Agar No. 3) was purchased from Oxoid Limited (Basingstoke, UK). Fast Green FCF and Nile Red dyes, porcine pepsin, porcine lipase, porcine pancreatin (8 × USP), porcine bile extract, HCl, NaOH, $CaCl_2$, Na_2CO_3, NaCl, KCl, KH_2PO_4, $MgCl_2(H_2O)_6$, $(NH_4)_2CO_3$, $MgSO_4$, Tris-HCl, SDS, bicinchoninic acid solution, cupric sulphate solution, acetic acid, Tris base, sodium dodecyl sulfate (SDS), glycine, and bovine serum albumin (BSA) were purchased from Sigma Aldrich (Milan, Italy). Absolute ethanol and methanol were purchased from J.T. Baker (Griesheim, Germany). Laemmli Sample Buffer 2×, β-mercaptoethanol, Mini-PROTEAN® TGX Stain-Free™ Precast Gels, Bio-Safe™ Coomassie G-250 Stain, and the protein standards for SDS-PAGE (Precision Plus Protein Standards, Kaleidoscope) were purchased from Bio-Rad Laboratories Inc. (Hercules, California, US). Deionized water (System advantage A10®, Millipore S.A.S, Molsheim, France) was used for all the analyses.

2.2 Oleogel preparation

WP aerogel particles were prepared as previously described [4]. Briefly, WP aqueous solutions (20% w/w) were adjusted at pH 5.7 and gelled at 85 °C for 15 min in sealed 50 mL plastic tubes. The obtained hydrogel was cooled and homogenized by using a high-speed mixer at 13,000 rpm for 3 min (Polytron PT-MR3000, Kinematica AG, Littau, Switzerland). The hydrogel particles were then dispersed in ethanol (0.1 g/mL), homogenized and collected by centrifugation at 13,000*g* for 10 min at 4 °C (Avanti J-25, Beckman, Palo Alto, CA, USA). This procedure was repeated twice to completely remove water. The ethanol was then removed using a supercritical-CO_2-drying plant at 60 °C and 120 bar. The dried particles were ground 1 min using a domestic grinder (MC3001, Moulinex, Milan, Italy) and dispersed into oil (0.1 g/mL), homogenized and collected by centrifugation, as previously described. This procedure was repeated twice, obtaining oleogels presenting 80% (w/w) oil content, whose complete characterization has been previously reported [4,5].

2.3 Powder solubility

The solubility of WP isolate and aerogel particles was assessed gravimetrically as reported by Melchior *et al*. [16]. Three aliquots of WP isolate or aerogel powder (W_0, 100 mg) were suspended in 1 mL deionized water (pH = 7.0 ± 0.2) and stirred 2 min at 37 °C. One aliquot was centrifuged at 15,000*g* for 5 min at 4 °C (D3024, DLAB Scientific Europe S.A.S, Schiltigheim, France). The supernatant and the precipitate were carefully separated. The insoluble precipitates were dried in a vacuum oven at 75 °C overnight (Vuotomatic 50, Bicasa, Milan, Italy) and weighted (W_1, mg). Powder solubility was expressed according to eq. 1:

$$Powder\ solubility\ (\%) = \frac{W_0 - W_1}{W_0} \cdot 100 \qquad \text{(eq. 1)}$$

The second and third aliquots were instead adjusted at pH 3.0 with HCl 1 M and stirred at 37 °C for 2 h. The solubility of the second aliquot was then determined; the third aliquot was adjusted to pH 8.0 with NaOH 1 M, further stirred at 37 °C for 2 h, and finally assessed for solubility.

2.4 *In vitro* digestion

In vitro digestion was carried out according to the INFOGEST static digestion protocol proposed by Brodkorb *et al*. [17]. Briefly, the simulated salivary (SSF), gastric (SGF) and intestinal (SIF)

fluids were prepared, stored at 4 °C and preheated to 37 °C just before *in vitro* digestion. Amylolytic enzymes were not considered due to the lack of carbohydrates in the digested matrices. The oral phase was started by adding to the sample 4 mL SSF, 25 μL 0.3 M $CaCl_2$, and 975 μL water. The sample was maintained at 37 °C under stirring for 2 min. At the end of the oral phase, 8 mL SGF, 5 μL 0.3 M $CaCl_2$, and 667 μL of an aqueous pepsin solution providing 2,000 U/mL activity in the final chyme, were added. To start the gastric phase, the pH was adjusted to 3.0 with 1 M HCl and the volume was made up to 20 mL with water. The mix was stirred at 37 °C for up to 2 h. At the end of the gastric phase, 8 mL SIF, 4 μL 0.3 M $CaCl_2$, 5 mL of a lipase-pancreatin solution, prepared in SIF and providing 2000 and 100 U/mL activity respectively in the final mixture, and 3 mL of 160 mM bile extract prepared in SIF were added. To start the intestinal phase, the pH was adjusted to 8.00 ± 0.10 with 1 M NaOH and the volume was made up to 40 mL with water. The mix was stirred at 37 °C for up to 2 h.

2.5 Lipid digestibility

For lipid digestibility trials, $NaHCO_3$ was replaced with NaCl in SSF, SGF and SIF as suggested for the pH-stat approach, which was used to determine the extent of lipid digestibility [18]. Immediately after the addition of lipase (paragraph 2.4), the pH of the digestion mixture was monitored and maintained at 8.00 ± 0.10 by adding 0.25 M NaOH. The choice of using pH 8.00 instead of 7.00 was based on the technical specifications of the used lipase. Based on oleogel composition (80% oil content), an oleogel amount of 1.25 g, corresponding to 1 g oil, was used, and the volume of NaOH (mL) added to titrate the oleogels was recorded ($V_{oleogel}$). An aliquot of lipid-free aerogel particles (0.25 g) corresponding to that contained in the oleogels was also digested to estimate the proteolysis contribution to pH lowering and the required NaOH volume registered ($V_{aerogel}$). Finally, the NaOH volume required to titrate unstructured SO and FLX oil (1 g) was also recorded (V_{oil}).

The percentage of free fatty acids (FFA) released during lipolysis was calculated according to eq 2:

$$\text{FFA}\ (\%) = \frac{V_e}{V_t} \times 100 \qquad \text{eq. 2}$$

where V_e is the experimental volume, represented by: (i) V_{oil} in the case of oils; (ii) the difference between $V_{oloegel}$ and $V_{aerogel}$ in the case of oleogels, based on the assumption that proteolysis is not affected by the presence of oil, as reported in literature studies aiming at optimizing the pH-stat approach on complex matrices containing oil and proteins [12,18]. V_t represents the theoretical volume required to titrate the fatty acids released by complete hydrolysis of triglycerides in the reaction vessel, assuming 2 FFA are produced for each triacylglycerol molecule [18], and was calculated according to eq. 3:

$$V_t = 2 \times \left[\frac{m_{oil}}{MW_{oil}} \frac{1000}{C_{NaOH}}\right] \qquad \text{eq. 3}$$

where m_{oil} is the mass of oil in the reaction vessel (g), MW_{oil} is the average molecular weight of SO (876.6 g mol^{-1}) and FLX (542.6 g mol^{-1}) oil and C_{NaOH} is the concentration of the sodium hydroxide (M). The maximum value of FFA released during digestion was determined after the *plateau* was reached, *i.e.*, after 30 min from the beginning of intestinal phase. This value was considered as an indication of the maximum lipolysis and was reported as FFA_{max}.

2.6 Protein digestibility

Protein digestibility trials were conducted on WP aerogel particles and native WP aqueous dispersions (used as control) (10%, w/w) prepared by stirring overnight at room temperature. At the end of gastric and intestinal phases, hydrolysis was stopped by adding ethanol (1:3 v/v). Samples were then centrifuged with a high-speed centrifuge (Avanti Centrifuge™ J-25, Beckman Coulter, Indianapolis, IN, USA) at 11,000*g* for 10 min at 4 °C. The supernatant and the precipitate were separated, and the precipitate (undigested fraction) was dried in a vacuum oven at 40 °C overnight (Vuotomatic 50, Bicasa, Milan, Italy), and stored in a desiccator containing P_2O_5 at room temperature until use.

2.6.1 Sodium Dodecyl Sulphate PolyAcrylamide Gel Electrophoresis (SDS-PAGE). SDS-PAGE was performed according to the method of Laemmli [19]. An amount of dried precipitate containing 3 mg of proteins (based on BCA assay, paragraph 2.6.2) was mixed with 500 µL of Laemmli Sample Buffer 2× in the presence of 10 µL of the reducing agent β-mercaptoethanol, incubated for 1 h at 20 °C, heated at 95 °C for 5 min, and centrifuged 10 min at 10,000g at 20 °C (Mikro 120, Hettich Italia S.r.l., Milan, Italy). Then, 10 µL of the prepared sample was loaded into SDS-PAGE pre-stained gels (Mini- PROTEAN® Tetra Cell apparatus, Bio-Rad, Hercules, CA, USA) and the electrophoresis was performed at 30 mA. The running buffer was made of 1.92 M glycine, 250-mM Tris base, and 1% SDS. Gels were then placed for 30 min in a gel-fixing solution (40%methanol and 10% acetic acid) and stained with Coomassie blue overnight. A bioanalytical imaging system (G:Box Chemi XX9, Syngene, Cambridge, UK) was used to see the protein lanes and the software GeneSys (Syngene, Cambridge, UK) was used to take the gel images. Protein identification was based on the comparison with protein standards in the molecular weight range 10-250 kDa.

2.6.2 Bicinchoninic acid (BCA) assay. The protein content in the dried precipitate was quantified with BCA assay according to Smith *et al.* [20], adapted to a 96-well microplate spectrophotometer procedure. This assay is based on the reaction of peptides containing three or more amino acid residues with cupric ion to form a colored chelate complex, spectrophotometrically detected [21]. BCA working reagent (WR) was prepared by mixing the bicinchoninic acid solution with the cupric sulphate solution (4% w/v) to reach the final ratio of 50:1. An extraction buffer (pH=7.5), prepared with Tris-HCl 60 mM and SDS (2 % w/v), was used to extract proteins from the dried precipitate fraction. Samples were diluted with water to reach the final concentration within the range of the calibration curve, prepared using bovine serum albumin (0-2000 µg/mL bovine serum albumin, $R^2 = 0.994$). Aliquots of 25 µL of diluted samples

were placed into a 96-well MicrotiterTM microplates (Thermo Fisher Scientific, Waltham, MA USA) and 200 µL of WR was added to each well. Samples were incubated in a microplate reader (Sunrise-Basic Tecan, Tecan GmbH, Grödig, Austria) at 37 °C for 30 min in the dark. Then the absorbance was measured at 562 nm and protein content (*P,* µg/mL) determined by comparison with the calibration curve. Digested proteins, i.e., free aminoacids and dipeptides, were computed by eq. 4:

$$Digested\ proteins\ (\%) = \frac{P_0 - P_I}{P_0} \times 100 \qquad \text{eq. 4}$$

where P_O is the protein content in the blank (undigested sample) and P_I is the protein content detected in the precipitate obtained after each digestion phase.

2.7 Confocal microscopy

A 0.2% aqueous solution of Fast Green and Nile Red was used to stain, respectively, the proteins and the oil. The hanging-drop method was used [22] to analyze samples collected after gastric and intestinal digestion phases. After staining, the samples were added with agarose (1% w/w), in a sample:agarose ratio of 1:2 (v/v). An amount of 2 µL of the obtained mix was placed on a microscope coverslip and left to set 1 min. The cover-slip with the gelled droplet was then fixed on a concave microscope slide and observed using a confocal laser scanning microscope at 100× magnification (Leica TCS SP8 X confocal system, Leica Microsystems, Wetzlar, Germany). Images were imported in jpeg format using the software LasX 3.5.5 (Leica Microsystems, Wetzlar, Germany). The mean oil droplet dimension was estimated based on the comparison with the scale bar.

2.8 Micelle size distribution

Digestate samples were collected at the end of the intestinal phase. The enzymatic hydrolysis was stopped by adding ethanol (sample:ethanol = 1:3, v/v). Samples were then centrifuged with a high-speed centrifuge (Avanti Centrifuge™ J-25, Beckman Coulter, Indianapolis, IN, USA) at 30,000*g* for 70 min at 4 °C. The supernatant was collected and immediately analyzed. The particle size distribution was measured by dynamic laser light scattering (DLS, Zetasizer NanoZS, Malvern Instruments, Worcestershire, UK). Samples were poured in plastic cuvettes, placed in the instrument cell and analyzed at 25 °C. The angle of observation was 173°. Solution refractive index and viscosity were set at 1.333 and 0.001 Pa·s, corresponding to the values of pure water at 25 °C. Particle mean diameter corresponding to volume distribution was calculated by Distribution Analysis fitting.

2.9 Data analysis

Determinations were expressed as the mean ± standard deviation of at least three repeated measurements from two experiment replicates. Statistical analysis was performed by using R v. 3.0.2 (The R Foundation for Statistical Computing). A one-way analysis of variance (ANOVA) was carried out to identify significantly different samples ($p < 0.05$).

3 Result and Discussion

3.1 Digestibility of WP-aerogel templated oleogels

Oleogels were obtained *via* absorption into the WP aerogel particles of SO and FLX oil, as described elsewhere [4,5]. The characterization of the oleogels is reported in our previous work [5]. The samples were *in vitro* digested to study lipid digestibility.

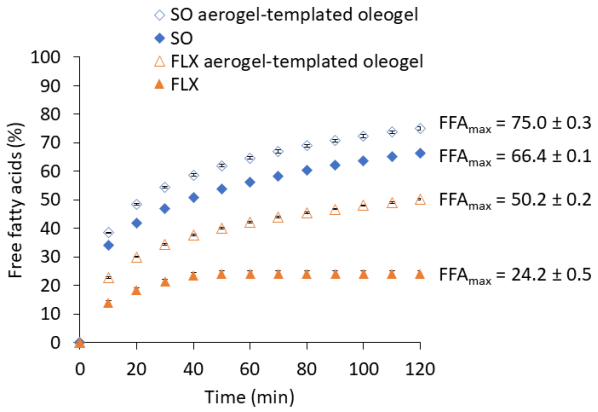

Figure 1 reports the percentage of free fatty acids (FFA) released during the intestinal *in vitro* digestion of SO and FLX oil oleogels and of the unstructured oils.

Figure 1. Percentage of free fatty acids released during *in vitro* intestinal digestion of unstructured sunflower (SO) and flaxseed (FLX) oil and of the corresponding whey protein aerogel-templated oleogels. Inset data reports the maximum lipolysis of the samples (FFA $_{max}$).

Typical profiles of FFA release during digestion were obtained, showing a faster rate in the first minutes followed by slower kinetics after an inflection point [12,18,23]. The FFA released after 2 h intestinal digestion was used to determine the maximal lipolysis (FFA$_{max}$), which resulted around 66 and 24% for SO and FLX oil, respectively. These results can be attributed to the different steric obstruction of the triglycerides of the two oils, affected by both the unsaturation degree and the average length of the fatty acid chains [8]. In this regard, FLX oil is rich in ω-3 polyunsaturated fatty acids [15]; whereas the fatty acid composition of SO oil is mainly represented by oleic and linoleic acid, followed by palmitic acid [24]. Oil structuring into the WP aerogel-templates led to an increase in the lipolysis degree, with FFA$_{max}$ values around 75 and 50% for SO and FLX oil, respectively (Figure 1). This result was quite surprising, since the presence of a network entrapping the oil has been previously reported to have the opposite effect of reducing oil susceptibility to digestion. For example, oleogelation with waxes, phytosterols, or monoglycerides resulted in a reduced lipolysis of high oleic sunflower oil and canola oil [25,26]. The obtained results could be explained based on the peculiar structure of the oleogels considered in this study, and on their

de-structuring behaviour during digestion. The microstructure of the digestate was thus analysed to gain a deep understanding of the complex interplay among protein aerogels and oil lipids under the digestive conditions. Figure 2 reports the confocal micrographs of the samples obtained after gastric and intestinal digestion of SO and FLX oil oleogels and of the corresponding unstructured oils.

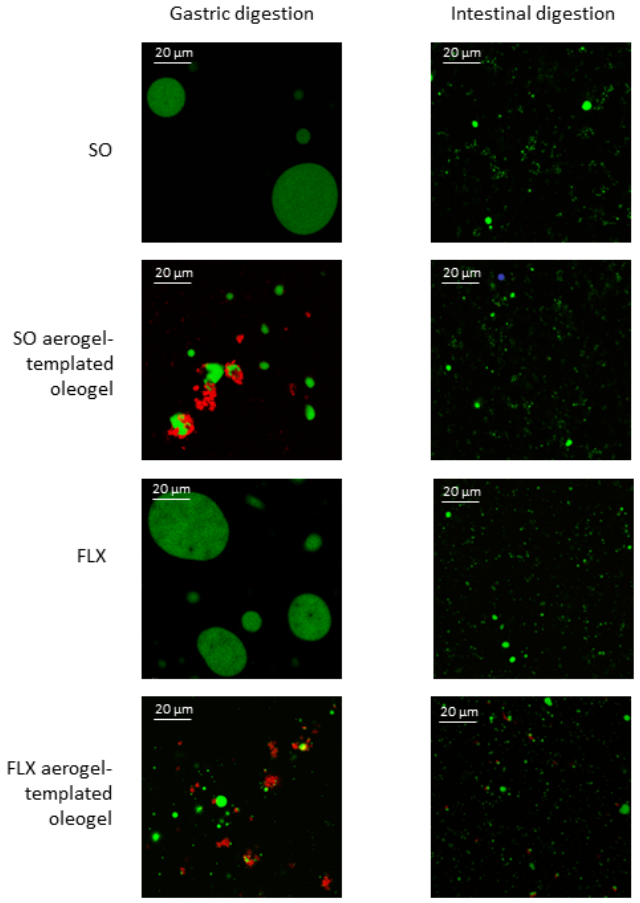

Figure 2. Confocal micrographs of the digestate samples obtained upon gastric and intestinal digestion of unstructured sunflower (SO) and flaxseed (FLX) oil and of the corresponding whey protein aerogel-templated oleogels. Green: oil; Red: proteins.

Upon gastric digestion, SO and FLX oil digested samples presented large droplets in the range 10-60 µm. This was expected, due to the immiscibility of oil with the aqueous gastric environment [14,27]. By contrast, upon the intestinal digestion, small and uniformly distributed oil droplets were observed for both the considered oils. This is due to the emulsifying action of bile salts, associated with the continuous mixing aiming at simulating peristaltic movements, which allow the breakage of the large oil droplets into smaller ones, easily attacked by the lipases [27]. Looking at the digestate structure of the oleogels, it can be noted that fractions of the original aerogel scaffold were still clearly evident upon the gastric phase (Figure 2), suggesting that the aerogelation of proteins led to a peculiar resistance to gastric proteolysis, confirming literature data [2]. In the gastric environment, the initial structure of the oleogel was partly lost with the formation of oil droplets having a maximal dimension lower than 20 µm (Figure 2). Many of these oil droplets were surrounded by WP aerogel particles. In this way, the oil was dispersed in droplets with lower size dimension as compared to those observed upon gastric digestion of the unstructured oils (Figure 2). Smaller particles would expose a larger surface for the action of lipases [23,28], possibly explaining why oil structuring by aerogel particles favoured the lipolysis in the small intestine (Figure 1). Moreover, aerogel particles were actually made of WP, which are commonly used surfactants. It cannot thus be excluded that WP aerogels acted as emulsifiers in the intestinal digestive mix, further favouring lipolysis. In this regard, a similar enhancement in lipolysis was also observed when oil was co-digested with monoglycerides, which are known to present a prominent surfactant activity [29]. The enhanced digestibility of the oil in the oleogel was further confirmed by analysing the dimension and distribution of digestive micelles (Figure 3).

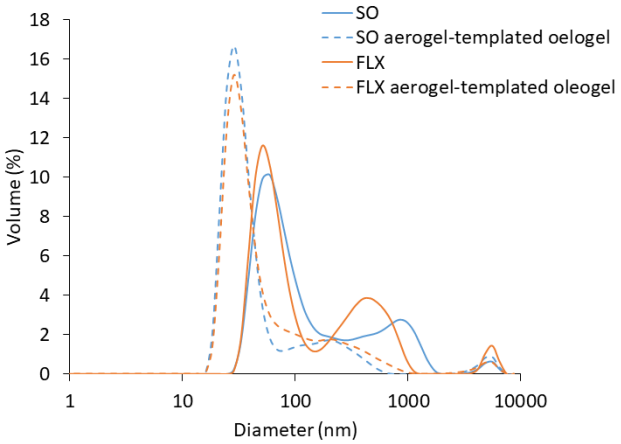

Figure 3. Particle size distribution of micelles obtained after *in vitro* intestinal digestion of unstructured sunflower (SO) and flaxseed (FLX) oil and of the corresponding whey protein aerogel-templated oleogels.

For both SO and FLX oil, the DLS profiles of the digestate fraction containing the micelles showed a tri-modal distribution. The prominent family, with dimension around 60 nm, is attributable to the mixed micelles formed upon digestion and representing the fraction that can be potentially absorbed through the intestinal epithelium [30]; the minor particle families at 530 and 5500 nm are instead probably represented by undigested lipid droplets [31,32]. In the case of oleogels, a three-peak distribution was still obtained but a shift towards smaller particle dimensions, associated with an increased frequency of the smaller-dimension families, was obtained for both the considered oils. Oil structuring within WP aerogels thus resulted in a modification of micelle dimension distribution at the intestinal level (Figure 3). Therefore, it can be inferred that WP aerogel-template oleogelation may play a role in determining the absorption of loaded lipophilic bioactive compounds. Such effect would depend on the de-structuring behaviour of

aerogel-templated oleogels, which delivered the oil in the intestine in the form of small particles surrounded and stabilized by surface active proteins, resistant to gastric digestion. Figure 2 actually shows that WP aerogels largely withstood the gastric digestion while being susceptible to the intestinal one. In fact, at the end of the intestinal digestion, only a few aerogel residues were detected (Figure 2). To confirm and quantify the effect of aerogelation on protein digestibility, the attention was then focused on WP aerogel de-structuring during simulated digestion. To this aim, the digestibility of lipid-free WP aerogels as compared to unstructured WP was assessed. Figure 4 reports the SDS-PAGE patterns of WP and WP aerogel particles before and after gastric and intestinal digestion.

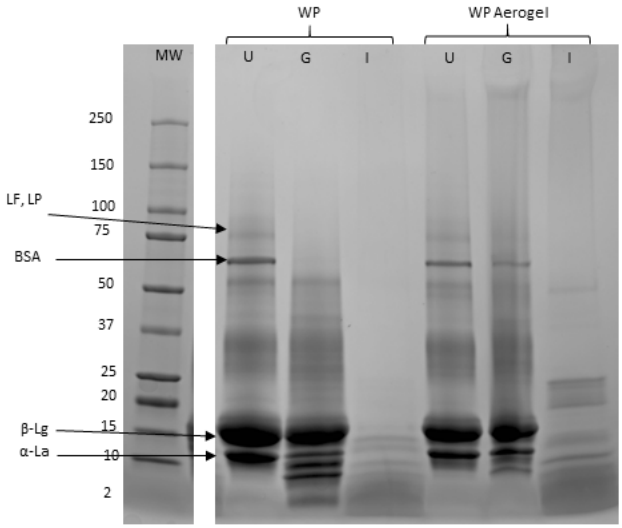

Figure 4. SDS-PAGE patterns of unstructured whey proteins (WP) and whey protein aerogels (WP Aerogel) before (undigested, U) and after gastric (G) and intestinal (I) digestion. MW: standard molecular weights, LF: lactoferrin, LP: lactoperoxidase, BSA: bovine serum albumin, α-La: α-lactalbumin, β-Lg: β-lactoglobulin.

Before digestion, both samples showed the presence of typical WP proteins [33]: β-lactoglobulin (β-Lg, 18 kDa), α-lactalbumin (α-La, 14 kDa), lactoferrin (LF) and lactoperoxidase (LP) (75 kDa), and bovine serum albumin (BSA, 70 kDa). The absence of bands at low molecular weight (<10 kDa) confirmed the absence of peptides before digestion. After the gastric digestion of WP, peptide bands were well evident, with the concomitant disappearance of high MW protein bands (LF, LP, BSA). Their absence clearly evidences that WP were mostly digested by gastric pepsin [34]. After the gastric phase, β-Lg and α-La bands were less pronounced but still present, confirming their higher hydrolysis resistance [34]. Only few peptide bands were present after the intestinal phase, indicating that most of the proteins were completely hydrolyzed to small peptides with molecular weight lower than 2 kDa. By contrast, after gastric hydrolysis of WP aerogels, the SDS-PAGE pattern showed the same protein bands of the undigested sample, even if less pronounced, along with a few peptide bands with MW in the range 2-10 kDa. This confirms that aerogelation increased protein resistance to peptic action, in agreement with literature findings [2]. During the production of WP aerogel particles used in this study, insoluble structures, called microgels, are formed by thermal coagulation near the isoelectric pH [4]. Microgels can be attacked by pepsin only at the surface [35] and their aerogelation further increases the WP digestive resistance by inducing protein clustering into large aggregates, which are probably not easily accessible to gastric enzymes [36]. Interestingly, low MW protein and peptide bands were detected after the intestinal digestion of WP aerogels, suggesting that the hydrolysis of the protein backbone only took place during this phase. This was initially attributed to the solubilization of the WP aerogels. However, differently from WP, which, as expected, resulted readily water soluble under oral digestion conditions (2 min, 37 °C, pH 7.0), WP aerogels showed an oral solubility around 10%, which did not increase even upon further exposure to gastro-intestinal conditions (2 h, 37 °C, pH 3.0 followed by 2 h, 37 °C, pH 8.0). The reduced WP aerogel solubility can be attributed to both exposure of hydrophobic surface induced by gelation and protein aggregation induced by solvent exchange and supercritical-CO_2-drying [36]. Despite the low solubility of aerogel proteins under the gastro-intestinal conditions, upon prolonged contact with water, they might swell and lose structural integrity [36], thus becoming more susceptible to the hydrolytic activity of proteases. Moreover, it cannot be excluded that the passage from stomach to intestine further destabilized the compact structure of the aerogel particles, possibly due to the burst pH shift, which can cause significant changes in protein spatial organization. In this regard, a significant effect of pH has been reported on the swelling kinetics and on the structural integrity of protein aerogels by Kleemann *et al.* [2]. The SDS-PAGE results were confirmed by the quantification of digested proteins with BCA assay (Figure 5).

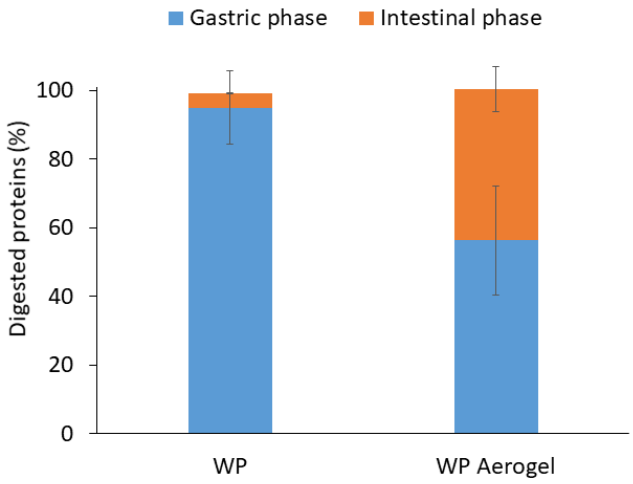

Figure 5. Digested proteins after gastric and intestinal digestion of unstructured whey protein (WP) and whey protein aerogel particles (WP Aerogel).

WP isolate was almost completely digested to dipeptides and free aminoacids after the gastric phase. By contrast, about 50% of the aerogel proteins resisted gastric hydrolysis and were subsequently digested in the intestine. In other words, despite the different susceptibility of WP and WP aerogel particles to simulated gastrointestinal conditions, at the end of the digestion, both samples resulted completely digested. Thus, the conversion of proteins into aerogels was not found to compromise the overall bioaccessibility of proteins, i.e., the fraction of small peptides and aminoacids that can be absorbed through the intestinal epithelium, thus becoming available for metabolic functions [37]. Rather, the aerogelation process allowed for a slower and more progressive release of bioaccessible peptides. This aspect appears interesting and valuable for further studies.

4 Conclusions

The peculiar destructing behaviour of WP aerogel-templated oleogels during gastro-intestinal digestion allows the loaded oil to be released in the small intestine in the form of a finely dispersed phase, possibly stabilised by undigested aerogel WP proteins at the oil droplet surface. As a result, the loaded oil is more susceptible to intestinal lipolysis resulting in a higher lipid digestibility, contrarily to what was generally observed when using other oil structuring agents. On the opposite, aerogelation increases the gastric resistance of WPs, which are digested into peptides only at the intestinal level.

The peculiar properties of aerogel-templated oleogels makes them promising candidates as fat replacers able not only to provide the required technological performances, but also to tune the digestibility of both the structured oil and the protein template.

From one side, this would be particularly interesting to deliver lipophilic bioactive molecules, such as polyunsaturated fatty acids here considered, and in the treatment of diseases characterized by a restrained fat absorption. On the other side, this approach could be used to modulate the release, stability, and functionality of bioactive peptides derived from WPs.

Author Contributions

Conceptualization SP SC LM, Data curation LDB, Formal analysis SP MA LDB, Investigation SP LDB, Methodology SP MA LDB SM, Project administration SC LM, Resources LM, Supervision SC LM, Visualization SP LDB, Writing - original draft SP, Writing - review and editing All the authors.

Conflicts of interest

There are no conflicts to declare.

Acknowledgements

This publication is based upon work from COST Action "Advanced Engineering of aeroGels for Environment and Life Sciences" (AERoGELS, ref. CA18125), supported by COST (European Cooperation in Science and Technology).

References

1. C. A. García-González, I. Smirnova, Use of supercritical fluid technology for the production of tailor-made aerogel particles for delivery systems. *J. Supercrit. Fluids* **79**, 152–158 (2013).
2. C. Kleemann, *et al.*, In-vitro-digestion and swelling kinetics of whey protein, egg white protein and sodium caseinate aerogels. *Food Hydrocoll.* **101**, 105534 (2020).
3. L. Manzocco, K. S. Mikkonen, C. A. García-González, Aerogels as porous structures for food applications: Smart ingredients and novel packaging materials. *Food Struct.* **28**, 100188 (2021).
4. S. Plazzotta, S. Calligaris, L. Manzocco, Structural characterization of oleogels from whey protein aerogel particles. *Food Res. Int.* **132**, 109099 (2020).
5. S. Plazzotta, *et al.*, Conversion of whey protein aerogel particles into oleogels: Effect of oil type on structural features. *Polym.* ***13****, 4063* (2021).
6. C. M. O'Sullivan, M. Davidovich-Pinhas, A. J. Wright, S. Barbut, A. G. Marangoni, Ethylcellulose oleogels for lipophilic bioactive delivery - effect of oleogelation on in vitro bioaccessibility and stability of beta-carotene. *Food Funct.* **8**, 1438–1451 (2017).
7. S. Y. Tan, E. Wan-Yi Peh, A. G. Marangoni, C. J. Henry, Effects of liquid oil vs. oleogel co-ingested with a carbohydrate-rich meal on human blood triglycerides, glucose, insulin and appetite. *Food Funct.* **8**, 241–249 (2017).
8. S. Y. Tan, E. Peh, P. C. Siow, A. G. Marangoni, C. J. Henry, Effects of the physical-form and the degree-of-saturation of oil on postprandial plasma triglycerides, glycemia and appetite of healthy Chinese adults. *Food Funct.* **8**, 4433–4440 (2017).
9. W. Limpimwong, T. Kumrungsee, N. Kato, N. Yanaka, M. Thongngam, Rice bran wax oleogel: A potential margarine replacement and its digestibility effect in rats fed a high-fat diet. *J. Funct. Foods* **39**, 250–256 (2017).
10. S. Calligaris, M. A. Alongi, P. Lucci, M. Anese, Effect of different oleogelators on lipolysis and curcuminoid bioaccessibility upon in vitro digestion of sunflower oil oleogels. *Food Chem.* **314**, 126146 (2020).
11. E. Bauer, S. Jakob, R. Mosenthin, Principles of physiology of lipid digestion. *Asian-Australasian J. Anim. Sci.* **18**, 282–295 (2005).
12. D. J. L. Mat, I. Souchon, C. Michon, S. Le Feunteun, Gastro-intestinal in vitro digestions of protein emulsions monitored by pH-stat: Influence of structural properties and interplay between proteolysis and lipolysis. *Food Chem.* **311**, 125946 (2020).
13. D. J. McClements, Y. Li, Structured emulsion-based delivery systems: Controlling the digestion and release of lipophilic food components. *Adv. Colloid Interface Sci.* **159**, 213–228 (2010).
14. M. Armand, *et al.*, Characterization of emulsions and lipolysis of dietary lipids in the human stomach. *Am. J. Physiol. - Gastrointest. Liver Physiol.* **266**, G372–G381 (1994).
15. A. Goyal, V. Sharma, N. Upadhyay, S. Gill, M. Sihag, Flax and flaxseed oil: an ancient medicine and modern functional food. *J. Food Sci. Technol.* **51**, 1633–1653 (2014).
16. S. Melchior, S. Calligaris, G. Bisson, L. Manzocco, Understanding the impact of moderate-intensity pulsed electric fields (MIPEF) on structural and functional characteristics of pea, rice and gluten concentrates. *Food Bioprocess Technol.* **13**, 2145–2155 (2020).
17. A. Brodkorb, *et al.*, INFOGEST static in vitro simulation of

gastrointestinal food digestion. *Nat. Protoc.* **14**, 991–1014 (2019).
18. D. J. L. Mat, S. Le Feunteun, C. Michon, I. Souchon, In vitro digestion of foods using pH-stat and the INFOGEST protocol: Impact of matrix structure on digestion kinetics of macronutrients, proteins and lipids. *Food Res. Int.* **88**, 226–233 (2016).
19. U. K. Laemmli, Cleavage of structural proteins during the assembly of the head of bacteriophage T4. *Nature* **227**, 680–685 (1970).
20. P. K. Smith, *et al.*, Measurement of protein using bicinchoninic acid. *Anal. Biochem.* **150**, 76–85 (1985).
21. K. J. Wiechelman, R. D. Braun, J. D. Fitzpatrick, Investigation of the bicinchoninic acid protein assay: identification of the groups responsible for color formation. *Anal. Biochem.* **175**, 231–237 (1988).
22. S. Gallier, K. C. Gordon, H. Singh, Chemical and structural characterisation of almond oil bodies and bovine milk fat globules. *Food Chem.* **132**, 1996–2006 (2012).
23. Y. Li, D. J. McClements, New mathematical model for interpreting pH-stat digestion profiles: Impact of lipid droplet characteristics on in vitro digestibility. *J. Agric. Food Chem.* **58**, 8085–8092 (2010).
24. E. J. Campbell, Sunflower oil. *J. Am. Oil Chem. Soc.* **60**, 387–392 (1983).
25. S. Calligaris, M. Alongi, P. Lucci, M. Anese, Effect of different oleogelators on lipolysis and curcuminoid bioaccessibility upon in vitro digestion of sunflower oil oleogels. *Food Chem.* **314**, 126146 (2020).
26. A. Ashkar, S. Laufer, J. Rosen-Kligvasser, U. Lesmes, M. Davidovich-Pinhas, Impact of different oil gelators and oleogelation mechanisms on digestive lipolysis of canola oil oleogels. *Food Hydrocoll.* **97**, 105218 (2019).
27. M. C. Carey, D. M. Small, C. M. Bliss, Lipid digestion and absorption. *Annu. Rev. Physiol.* **45**, 651–677 (1983).
28. L. Dong, *et al.*, In vitro gastrointestinal digestibility of phytosterol oleogels: Influence of self-assembled microstructures on emulsification efficiency and lipase activity. *Food Funct.* **11**, 9503–9513 (2020).
29. P. Reis, *et al.*, Competition between lipases and monoglycerides at interfaces. *Langmuir* **24**, 7400–7407 (2008).
30. L. Salvia-Trujillo, *et al.*, Lipid digestion, micelle formation and carotenoid bioaccessibility kinetics: Influence of emulsion droplet size. *Food Chem.* **229**, 653–662 (2017).
31. L. Salvia-Trujillo, C. Qian, O. Martín-Belloso, D. J. McClements, Influence of particle size on lipid digestion and β-carotene bioaccessibility in emulsions and nanoemulsions. *Food Chem.* **141**, 1472–1480 (2013).
32. H. Singh, A. Ye, D. Horne, Structuring food emulsions in the gastrointestinal tract to modify lipid digestion. *Prog. Lipid Res.* **48**, 92–100 (2009).
33. F. F. Costa, *et al.*, Microfluidic chip electrophoresis investigation of major milk proteins: study of buffer effects and quantitative approaching. *Anal. Methods* **6**, 1666–1673 (2014).
34. R. Sousa, R. Portmann, S. Dubois, I. Recio, L. Egger, Protein digestion of different protein sources using the INFOGEST static digestion model. *Food Res. Int.* **130**, 108996 (2020).
35. A. Maclerzanka, *et al.*, The effect of gel structure on the kinetics of simulated gastrointestinal digestion of bovine β-lactoglobulin. *Food Chem.* **134**, 2156–2163 (2012).
36. L. Manzocco, *et al.*, Structural characterisation and sorption capability of whey protein aerogels obtained by freeze-drying or supercritical drying. *Food Hydrocoll.* **122**, 107117 (2022).
37. M. G. Ferruzzi, The influence of beverage composition on delivery of phenolic compounds from coffee and tea. *Physiol. Behav.* **100**, 33–41 (2010).

